

Figure S1. Hrr25-5 is defective in kinase activity. (A) Purified recombinant His₆-Hrr25 or His₆-Hrr25-5 were incubated with GST-Lst1, as described above. GST-Lst1 migrates slower when incubated with His₆-Hrr25 (compare lanes 1 and 2). The decrease in mobility is caused by phosphorylation as GST-Lst1 migrated faster (compare lanes 2 and 3) after it was treated with CIP. In contrast, GST-Lst1 incubated with His₆-Hrr25-5 did not change mobility after CIP treatment (compare lanes 4 and 5). (B) Western blot analysis was performed with WT and *hrr25-5* S1 fractions to detect the level of COPII coat proteins. Bos1 was used as a loading control. (C) Sec13-GFP, a subunit of the COPII coat, is recruited normally to ER membranes in the *hrr25-5* mutant. Cells (SFNY2397 and SFNY2398) were grown at 25°C and either examined immediately or shifted to 37°C for 1 h. Representative shifted cells are shown. 300 cells were examined in three separate experiments. The DIC image is on the right. Bar, 2 μm. (D) The localization of Hrr25 is not altered in a *ypt1-3* mutant at 25°C. Lysates (T) were prepared from WT and the *ypt1-3* mutant grown at 25°C and fractionated into supernatant (S) and pellet (P) fractions. The SNARE Bos1 was used as a fractionation control. (E) Coomassie-stained gels of samples shown in Fig. 3 A. (F) Coomassie-stained gels of samples shown in Fig. 3 B.

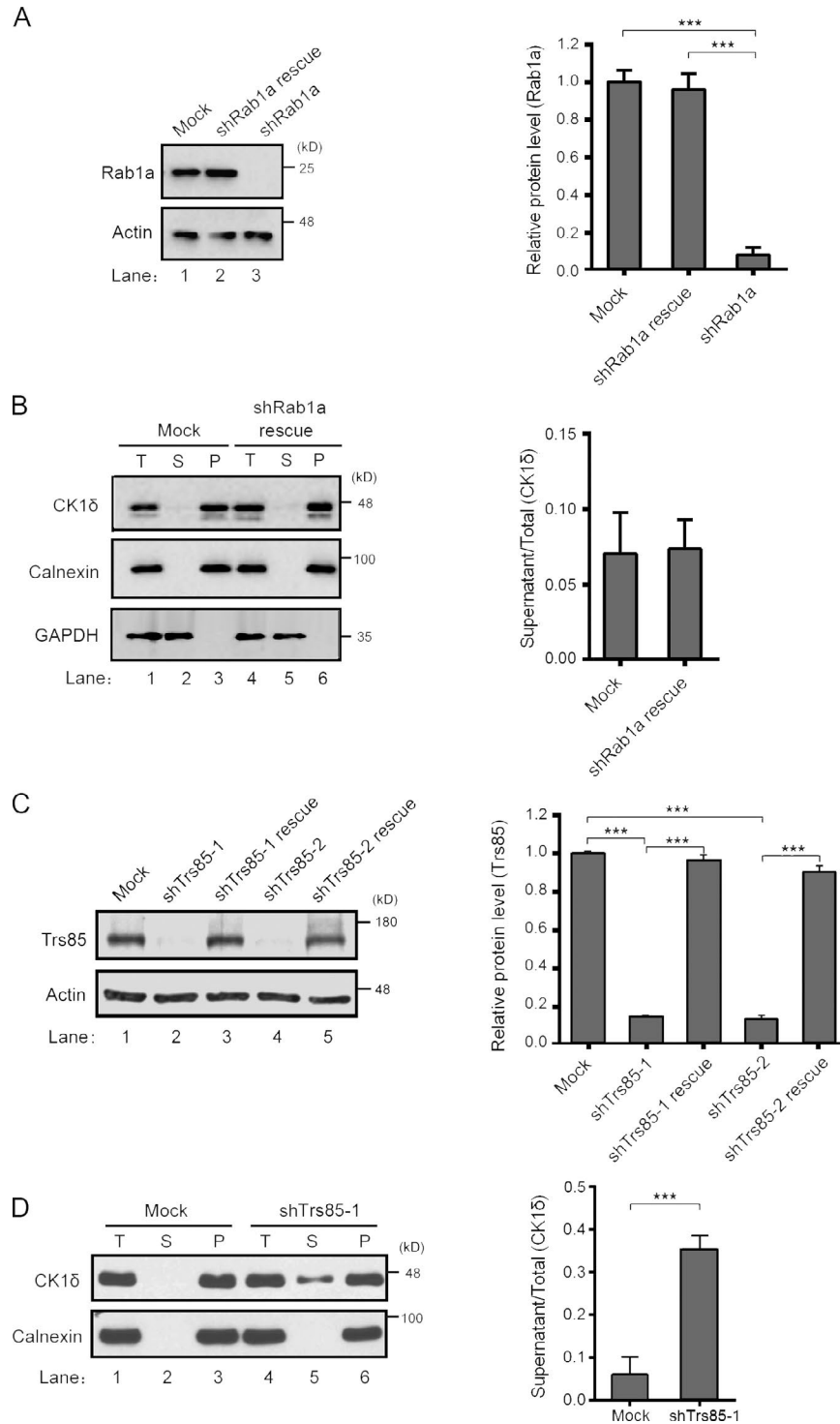


Figure S2. Failure to activate Rab1 leads to an increase in the soluble pool of CK1 δ . (A, left) HeLa cells were harvested 96 h after they were mock transfected or transfected with the shRab1 or the shRab1 rescue construct. Samples were immunoblotted with anti-Rab1 and anti-actin antibodies. Actin was used as a loading control. (A, right) Quantitation of immunodepletion experiments. Error bars represent SEM; $n = 3$; $***, P < 0.001$, Student's t test. (B, left) Lysates (T) were prepared from mock and shRab1a rescue cells and fractionated as previously described (Bhandari et al., 2013) to produce supernatant (S) and pellet (P) fractions. Western blot analysis was performed to detect CK1 δ , calnexin, and GAPDH in each fraction. (B, right) The ratio of CK1 δ in supernatant and total fractions was quantitated. (C, left) 2 d after shTrs85-1 and shTrs85-2 were transfected into HeLa cells, the cells were transfected with the shRNA-resistant constructs, and then harvested 48 h later. The knockdown and complementation efficiency was analyzed by Western blot analysis. Actin was used as a loading control. (C, right) The bar graphs show the relative protein levels of Trs85 that was quantitated. Error bars represent SEM; $n = 3$; $***, P < 0.001$, Student's t test. (D, left) Same fractionation protocol as B, Western blot analysis was performed to detect CK1 δ and calnexin in each fraction. (D, right) The ratio of CK1 δ in supernatant and total fractions was quantitated. Error bars represent SEM; $n = 4$; $***, P < 0.001$, Student's t test.

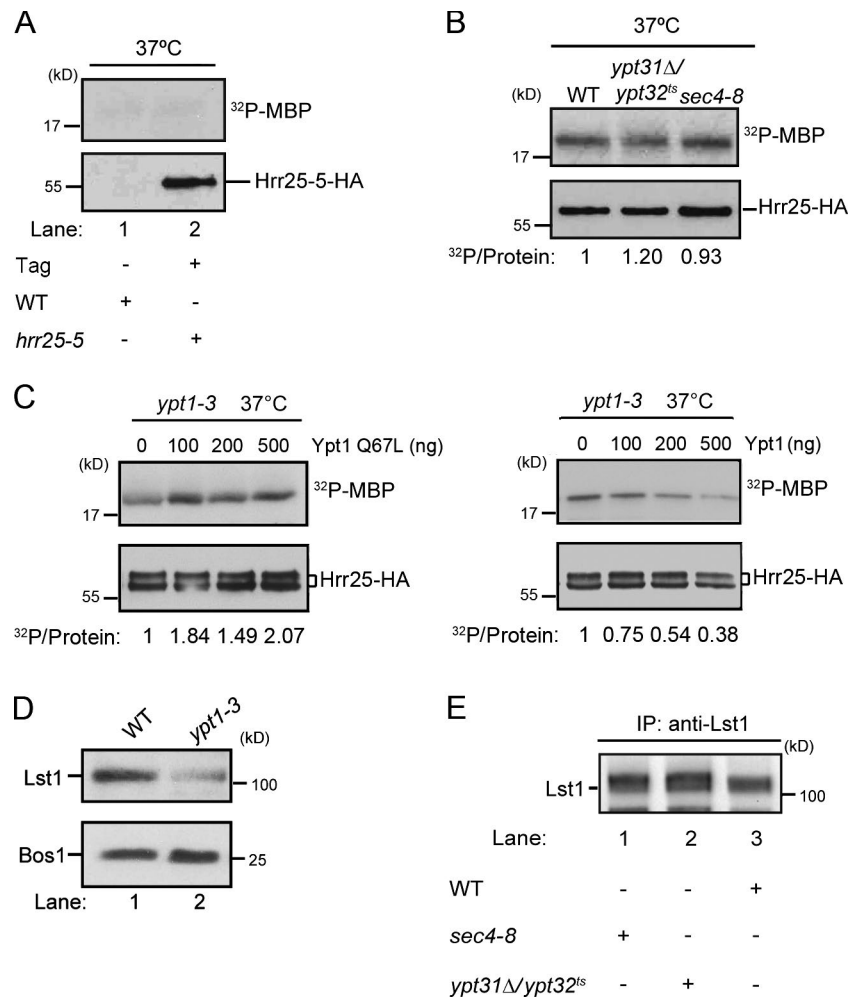


Figure S3. **Ypt1 regulates the phosphorylation of the COPII coat.** (A) Hrr25 was precipitated from untagged WT (lane 1; SFNY 2494) and the *hrr25-5* (lane 2) mutant (Hrr25-5-HA; SFNY2648) and then assayed for kinase activity. (B) Hrr25-HA was precipitated from WT (SFNY 2639) and the *ypt32Δypt31^{ts}* (SFNY 2646) and *sec4-8* (SFNY 2640) mutants after a 2-h shift to 37°C and assayed for kinase activity. Note that the kinase activity of WT is set to 1.0. (C) Activated Ypt1 (left), but not WT Ypt1 (right), partially restores kinase activity to Hrr25-HA isolated from the *ypt1-3* mutant. The same as Fig. 4 (C and D), except Hrr25-HA was precipitated from *ypt1-3* mutant cells that were incubated at 37°C for 2 h. The assays were performed multiple times. The data that is shown is representative. (D) Lst1 is unstable in the *ypt1-3* mutant. WT and *ypt1-3* mutant cells were shifted to 37°C for 2 h and an S1 fraction was prepared as previously described (Groesch et al., 1990; Lian and Ferro-Novick, 1993). (E) The loss of Sec4 or Ypt31/Yp32 function does not affect the mobility of Lst1. Same as Fig. 4 E, except Lst1 was precipitated from the *sec4-8* (NY 405) and *ypt32Δypt31^{ts}* (NY 2770) mutants after a 1-h shift to 37°C.

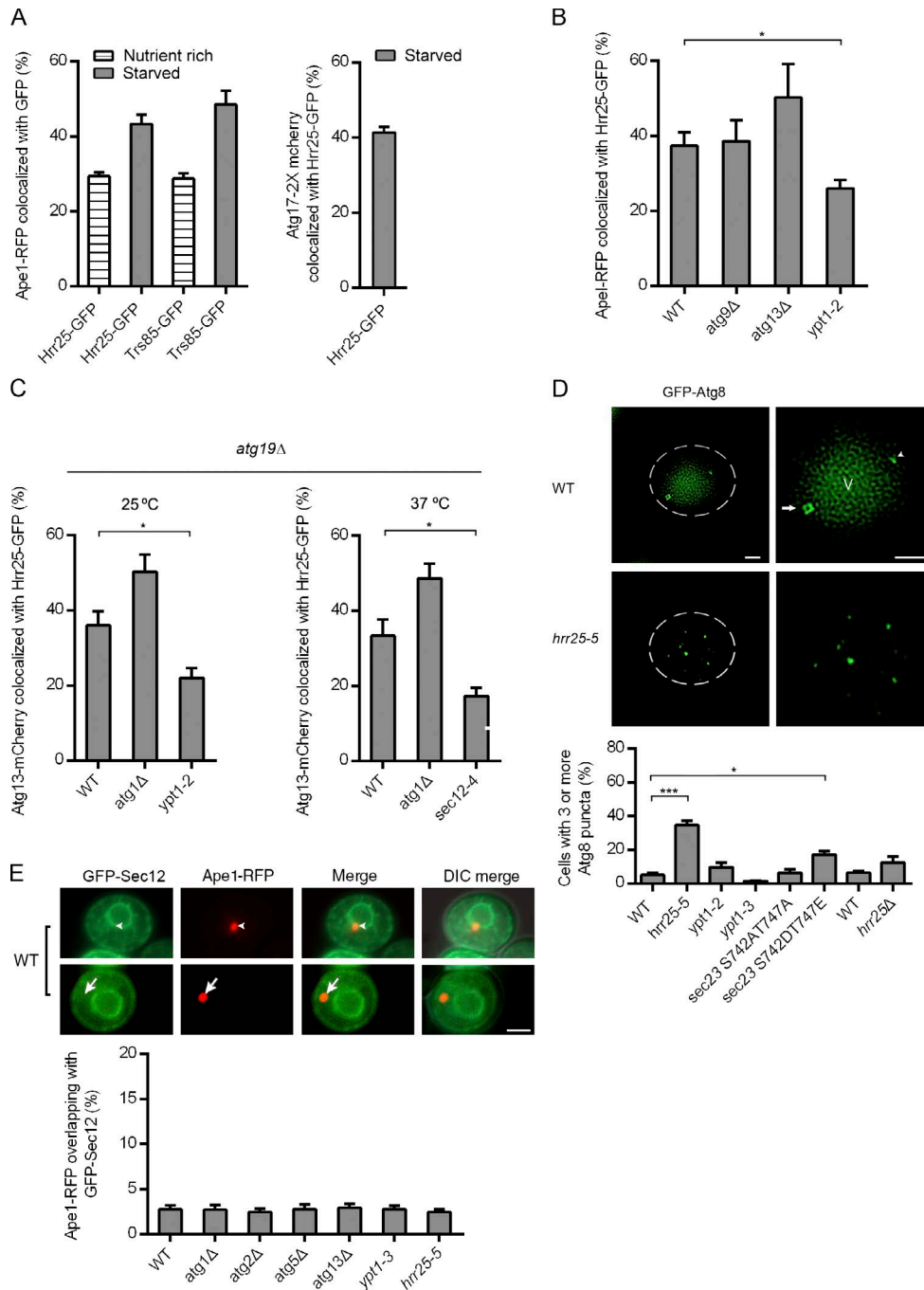


Figure S4. Hrr25 is recruited to the PAS. (A, left) Hrr25-GFP is recruited to the PAS. SFNY2527 and SFNY2573 cells expressing Ape1-RFP and Hrr25-GFP or Ape1-RFP and Trs85-3X GFP were grown to log phase in SC-Leu medium at 25°C (nutrient rich), and then shifted to SD-N medium at 25°C for 4 h (starved). (right) SFNY2572 cells expressing Atg17-2X-mCherry and Hrr25-GFP were grown to log phase in SC-Leu medium at 25°C and then shifted to SD-N medium at 25°C for 4 h (starved). Cells from three separate experiments (450 total) were used to calculate the percent of cells that contain colocalized Ape1-RFP and Hrr25-GFP or Ape1-RFP and Trs85-3X GFP. Starved cells from three separate experiments (450 total) were used to calculate the percent of cells that contain colocalized Atg17-2X-mCherry and Hrr25-GFP. Error bars represent SEM. (B) Same as Fig. 5 B only *atg9Δ* and *atg13Δ* were examined. Error bars represent SEM; $n = 3$; *, $P < 0.05$, Student's t test. (C) Same as Fig. 5 B, except all strains examined (SFNY2642, SFNY2643, SFNY2644, and SFNY2645) were deleted for *atg19Δ*. Error bars represent SEM; $n = 3$; *, $P < 0.05$, Student's t test. (D, top) WT (SFNY 2623) and *hrr25-5* (SFNY 2622) cells expressing GFP-Atg8 were grown to log phase at 25°C, and then shifted to SD-N medium before they were examined by fluorescence microscope. The deconvolved images are shown. Arrow, autophagosome; arrowhead, phagophore; V, vacuole. Bar, 1 μ m. (bottom) Cells from three separate experiments (450 total) were examined to calculate the percent of cells with 3 or more GFP-Atg8 puncta. Note that the *hrr25-5*, *ypt1-2*, *ypt1-3*, and *sec23* mutants are in the S288C strain background, whereas the *hrr25Δ* mutant is in the W303 strain background. The residual kinase activity in the *hrr25-5* mutant may contribute to the accumulation of Atg8 puncta. Error bars represent SEM; $n = 3$; *, $P < 0.05$; ***, $P < 0.001$, Student's t test. (E) Cells expressing GFP-Sec12 and Ape1-RFP were grown to log phase in SC-Leu medium at 25°C and then macroautophagy was induced for 2 h at 37°C. (top row) Images of WT cells. Arrowhead, Ape1-RFP puncta that overlaps with GFP-Sec12 on the nuclear ER. (bottom row) Arrow, Ape1-RFP puncta that does not overlap with the cortical or nuclear ER. Bar, 2 μ m. (bottom) Cells from three separate experiments (900 total) were examined to calculate the percentage of Ape1-RFP puncta that overlap with GFP-Sec12.

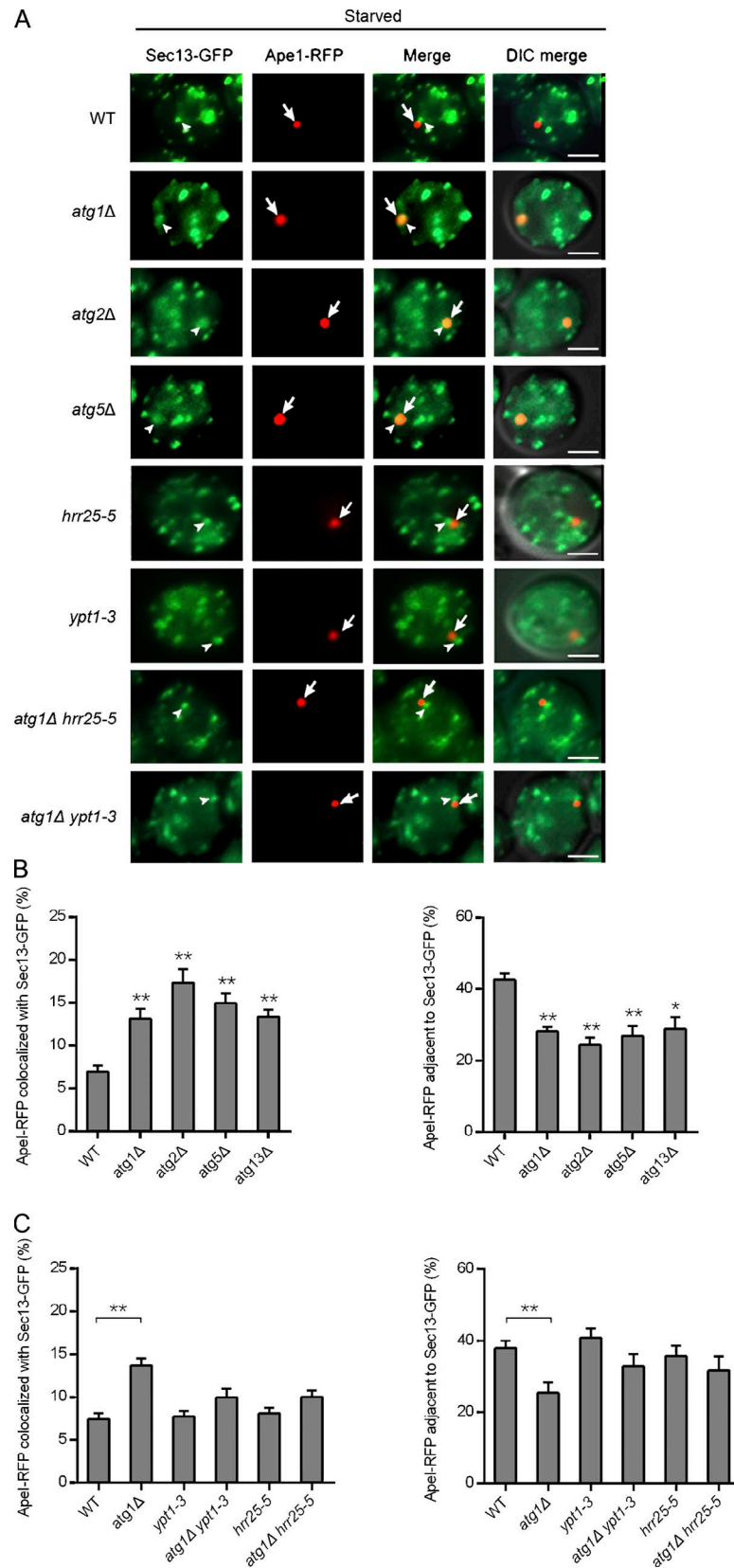


Figure S5. Hrr25 and Ypt1 are required for the accumulation of COPII vesicles at the PAS in *atg1Δ* mutants. The same as Fig. 6 G only log phase cells were shifted to SD–N medium. Images are shown in A. Arrowheads, Sec13-GFP puncta; arrows, Ape1-RFP. Bar, 2 μ m. (B) Quantitation of the percent of Ape1-RFP puncta that colocalize with (left) or lie adjacent to (right) Sec13-GFP puncta in WT and *atg1Δ* mutants shifted to SD–N medium at 25°C for 2 h. Error bars represent SEM; $n = 3$; *, $P < 0.05$; **, $P < 0.01$, Student's t test. (C) Same as B, except WT, *atg1Δ*, *hrr25-5* (SFNY 2666), *ypt1-3* (SFNY2667), *hrr25-5atg1Δ* (SFNY 2702), and *ypt1-3atg1Δ* (SFNY 2703) double mutants were grown to log phase in SC–Leu medium at 25°C and then shifted to SD–N medium at 37°C for 2 h before the cells were examined by fluorescence microscopy. Error bars represent SEM; $n = 3$; **, $P < 0.01$, Student's t test.

Table S1. Yeast strains used in this study

Strain no.	Genotype	Source
SFNY92	<i>MATα ura3-52 his4-619 bet2-1 pRB58 (URA3 SUC2 2μ)</i>	Ferro-Novick Lab Collection
SFNY445	<i>MATα ura3-52 leu2-3,112</i>	Ferro-Novick Lab Collection
SFNY446	<i>MATα ura3-52 ypt1-3</i>	Ferro-Novick Lab Collection
SFNY1950	<i>MATα ade2-101oc his3-Δ200 leu2-Δ1 lys2-801am trp1-Δ63 ura3-52 sec23Δ::His3MX6 pCF364 (TRP1 SEC23 CEN)</i>	Ferro-Novick Lab Collection
SFNY1951	<i>MATα ade2-101oc his3-Δ200 leu2-Δ1 lys2-801am trp1-Δ63 ura3-52 sec23Δ::His3MX6 pSFNB1749 (TRP1 sec23 S742A/T747A CEN)</i>	Ferro-Novick Lab Collection
SFNY1952	<i>MATα ade2-101oc his3-Δ200 leu2-Δ1 lys2-801am trp1-Δ63 ura3-52 sec23Δ::His3MX6 pSFNB1750 (TRP1 sec23 S742D/T747E CEN)</i>	Ferro-Novick Lab Collection
SFNY2049	<i>MATα his3Δ1 leu2Δ0 ura3Δ0 met15Δ0 hrr25Δ::KanMX6 pSFNB 1871 (LEU2 hrr25-5 CEN)</i>	Ferro-Novick Lab Collection
SFNY2051	<i>MATα his3Δ1 leu2Δ0 ura3Δ0 met15Δ0 hrr25Δ::KanMX6 pSFNB1715 (LEU2 HRR25 CEN)</i>	Ferro-Novick Lab Collection
SFNY2329	<i>MATα ura3-52 leu2-3,112 his3-Δ200 hrr25Δ::His3MX6 pSFNB1871 (LEU2 hrr25-5 CEN) pRB58 (URA3 SUC2 2μ)</i>	Ferro-Novick Lab Collection
SFNY2330	<i>MATα ura3-52 leu2-3,112 his3-Δ200 hrr25Δ::His3MX6 pSFNB1715 (LEU2 HRR25 CEN) pRB58 (URA3 SUC2 2μ)</i>	Ferro-Novick Lab Collection
SFNY2397	<i>MATα his3Δ1 leu2Δ0 ura3Δ0 met15Δ0 hrr25Δ::KanMX6 SEC13-GFP::URA3 pSFNB1715 (LEU2 HRR25 CEN)</i>	This study
SFNY2398	<i>MATα his3Δ1 leu2Δ0 ura3Δ0 met15Δ0 hrr25Δ::KanMX6 SEC13-GFP::URA3 pSFNB1871 (LEU2 hrr25-5 CEN)</i>	This study
SFNY2443	<i>MATα ura3-52 leu2-3,112 pBY924 (URA HRR25-HA CEN)</i>	This study
SFNY2445	<i>MATα ura3-52 ypt1-3 pBY924 (URA HRR25-HA CEN)</i>	This study
SFNY2488	<i>MATα his3-200 leu2-3,112 ura3-52 atg1Δ::His3MX6</i>	Ferro-Novick Lab Collection
SFNY2494	<i>MATα ura3-1 his3-11,15 trp1-1 leu2-3,112 ade2-1 can1-100</i>	Ferro-Novick Lab Collection
SFNY2520	<i>MATα his3-200 leu2-3,112 ura3-52 pBY924 (URA HRR25-HA CEN) pSFNB1602 (LEU2 ypt1 Q67L CEN)</i>	This study
SFNY2521	<i>MATα his3-200 leu2-3,112 ura3-52 pBY924 (URA HRR25-HA CEN) pSFNB2195 (LEU2 ypt1 S22N CEN)</i>	This study
SFNY2527	<i>MATα his3-200 leu2-3,112 ura3-52 HRR25-GFP::His3MX6 pSFNB2193 (LEU2 APE1-RFP CEN)</i>	This study
SFNY2528	<i>MATα his3-200 leu2-3,112 ura3-52 ypt1-2 HRR25-GFP::His3MX6 pSFNB2193 (LEU2 APE1-RFP CEN)</i>	This study
SFNY2529	<i>MATα his3Δ1 leu2Δ0 ura3Δ0 met15Δ0 hrr25Δ::KanMX6 pho8::pho8Δ60 pSFNB1715 (LEU2 HRR25 CEN)</i>	This study
SFNY2530	<i>MATα his3Δ1 leu2Δ0 ura3Δ0 met15Δ0 hrr25Δ::KanMX6 pho8::pho8Δ60 pSFNB1871 (LEU2 hrr25-5 CEN)</i>	This study
SFNY2554	<i>MATα ade2-101oc his3-Δ200 leu2-Δ1 lys2-801am trp1-Δ63 ura3-52 sec23Δ::His3MX6 pho8::pho8Δ60 pCF364 (TRP1 SEC23 CEN)</i>	This study
SFNY2555	<i>MATα ade2-101oc his3-Δ200 leu2-Δ1 lys2-801am trp1-Δ63 ura3-52 sec23Δ::His3MX6 pho8::pho8Δ60 pSFNB1749 (TRP1 sec23 S742A/T747A CEN)</i>	This study
SFNY2556	<i>MATα ade2-101oc his3-Δ200 leu2-Δ1 lys2-801am trp1-Δ63 ura3-52 sec23Δ::His3MX6 pho8::pho8Δ60 pSFNB1750 (TRP1 sec23 S742D/T747E CEN)</i>	This study
SFNY2565	<i>MATα ura3-52 ypt1-3 pho8::pho8Δ60</i>	This study
SFNY2567	<i>MATα his3-200 leu2-3,112 ura3-52 ypt1-2 pho8::pho8Δ60</i>	Ferro-Novick Lab Collection
SFNY2568	<i>MATα ura3-52 HRR25-GFP::KanMX6 pSFNB2194 (URA3 APE1-RFP CEN)</i>	This study
SFNY2569	<i>MATα ura3-52 sec12-4 HRR25-GFP::KanMX6 pSFNB2194 (URA3 APE1-RFP CEN)</i>	This study
SFNY2572	<i>MATα his3-200 leu2-3,112 ura3-52 HRR25-GFP::His3MX6 ATG17-2x mCherry:: LEU2</i>	This study
SFNY2573	<i>MATα his3-200 leu2-3,112 ura3-52 TRS85-3x GFP::URA3 pSFNB2193 (LEU2 APE1-RFP CEN)</i>	This study
SFNY2622	<i>MATα his3Δ1 leu2Δ0 ura3Δ0 met15Δ0 hrr25Δ::KanMX6 pSFNB1871 (LEU2 hrr25-5 CEN) pSFNB1637 (URA3 GFP-ATG8 CEN)</i>	This study
SFNY2623	<i>MATα his3Δ1 leu2Δ0 ura3Δ0 met15Δ0 hrr25Δ::KanMX6 pSFNB1715 (LEU2 HRR25 CEN) pSFNB1637 (URA3 GFP-ATG8 CEN)</i>	This study
SFNY2624	<i>MATα ade2-101oc his3-Δ200 leu2-Δ1 lys2-801am trp1-Δ63 ura3-52 sec23Δ::His3MX6 pSFNB1637 (URA3 GFP-ATG8 CEN) pCF364 (TRP1 SEC23 CEN)</i>	This study
SFNY2625	<i>MATα ade2-101oc his3-Δ200 leu2-Δ1 lys2-801am trp1-Δ63 ura3-52 sec23Δ::His3MX6 pSFNB1637 (URA3 GFP-ATG8 CEN) pSFNB1749 (TRP1 sec23 S742A/T747A CEN)</i>	This study
SFNY2626	<i>MATα ade2-101oc his3-Δ200 leu2-Δ1 lys2-801am trp1-Δ63 ura3-52 sec23Δ::His3MX6 pSFNB1637 (URA3 GFP-ATG8 CEN) pSFNB1750 (TRP1 sec23 S742D/T747E CEN)</i>	This study
SFNY2627	<i>MATα his3-200 leu2-3,112 ura3-52 SEC13-GFP::URA3 pSFNB2193 (LEU2 APE1-RFP CEN)</i>	Ferro-Novick Lab Collection
SFNY2628	<i>MATα his3-200 leu2-3,112 ura3-52 atg1Δ::His3MX6 SEC13-GFP::URA3 pSFNB2193 (LEU2 APE1-RFP CEN)</i>	Ferro-Novick Lab Collection
SFNY2629	<i>MATα his3-200 leu2-3,112 ura3-52 atg13Δ::His3MX6 SEC13-GFP::URA3 pSFNB2193 (LEU2 APE1-RFP CEN)</i>	Ferro-Novick Lab Collection
SFNY2639	<i>MATα ura3-52 pBY924 (URA HRR25-HA CEN)</i>	This study
SFNY2640	<i>MATα ura3-52 sec4-8 pBY924 (URA HRR25-HA CEN)</i>	This study

Table S1. Yeast strains used in this study (Continued)

Strain no.	Genotype	Source
SFNY2642	<i>MATα his3-200 leu2-3,112 ura3-52 atg19Δ::URA3 HRR25-GFP::KanMX6 pSFNB2221 (LEU2 ATG13-mCherry CEN)</i>	This study
SFNY2643	<i>MATα his3-200 leu2-3,112 ura3-52 atg19Δ::URA3 atg1Δ::His3MX6 HRR25-GFP::KanMX6 pSFNB2221 (LEU2 ATG13-mCherry CEN)</i>	This study
SFNY2644	<i>MATα his3-200 leu2-3,112 ura3-52 ypt1-2 atg19Δ::URA3 HRR25-GFP::KanMX6 pSFNB2221 (LEU2 ATG13-mCherry CEN)</i>	This study
SFNY2645	<i>MATα ura3-52 leu2-3,112 trp1 his4 sec12-4 atg19Δ::URA3 HRR25-GFP::KanMX6 pSFNB2221 (LEU2 ATG13-mCherry CEN)</i>	This study
SFNY2646	<i>MATα ura3-52 leu2-3,112 his3-Δ200 ypt31Δ::His3MX6 ypt32ts pBY924 (URA HRR25-HA CEN)</i>	This study
SFNY2648	<i>MATα ura3-1 his3-11,15 trp1-1 leu2-3,112 ade2-1 can1-100 hrr25Δ::His3MX6 pSFNB2223 (LEU2 hrr25-5-HA CEN)</i>	This study
SFNY2660	<i>MATα his3-200 leu2-3,112 ura3-52 ypt1-2 pSFNB1637 (URA3 GFP-ATG8 CEN)</i>	This study
SFNY2662	<i>MATα ura3-52 ypt1-3 pSFNB1637 (URA3 GFP-ATG8 CEN)</i>	This study
SFNY2663	<i>MATα ura3-1 his3-11,15 trp1-1 leu2-3,112 ade2-1 can1-100 pSFNB1637 (URA3 GFP-ATG8 CEN)</i>	This study
SFNY2664	<i>MATα ura3-1 his3-11,15 trp1-1 leu2-3,112 ade2-1 can1-100 hrr25::His3MX6 pSFNB1637 (URA3 GFP-ATG8 CEN)</i>	This study
SFNY2666	<i>MATα his3Δ1 leu2Δ0 ura3Δ0 met15Δ0 hrr25Δ::KanMX6 SEC13-GFP::URA3 APE1-RFP::His3MX6 pSFNB1871 (LEU2 hrr25-5 CEN)</i>	This study
SFNY2667	<i>MATα his3-200 leu2-3,112 ura3-52 ypt1-3 SEC13-GFP::URA3 pSFNB2193 (LEU2 APE1-RFP CEN)</i>	This study
SFNY2668	<i>MATα ura3-1 his3-11,15 trp1-1 leu2-3,112 ade2-1 can1-100 pSFNB1637 (URA3 GFP-ATG8 CEN) pSFNB2193 (LEU2 APE1-RFP CEN)</i>	This study
SFNY2669	<i>MATα ura3-1 his3-11,15 trp1-1 leu2-3,112 ade2-1 can1-100 hrr25::His3MX6 pSFNB1637 (URA3 GFP-ATG8 CEN) pSFNB2193 (LEU2 APE1-RFP CEN)</i>	This study
SFNY2670	<i>MATα his3-200 leu2-3,112 ura3-52 pSFNB1637 (URA3 GFP-ATG8 CEN) pSFNB2193 (LEU2 APE1-RFP CEN)</i>	This study
SFNY2671	<i>MATα his3-200 leu2-3,112 ura3-52 ypt1-3 pSFNB1637 (URA3 GFP-ATG8 CEN) pSFNB2193 (LEU2 APE1-RFP CEN)</i>	This study
SFNY2696	<i>MATα his3Δ1 leu2Δ0 ura3Δ0 met15Δ0 hrr25Δ::KanMX6 APE1-RFP::His3MX6 pSFNB1871 (LEU2 hrr25-5 CEN) pSFNB1637 (URA3 GFP-ATG8 CEN)</i>	This study
SFNY2697	<i>MATα his3-200 leu2-3,112 ura3-52 pLMB74 (URA3 GFP-SEC12 CEN) pSFNB2193 (LEU2 APE1-RFP CEN)</i>	This study
SFNY2698	<i>MATα his3-200 leu2-3,112 ura3-52 atg1Δ::His3MX6 pLMB74 (URA3 GFP-SEC12 CEN) pSFNB2193 (LEU2 APE1-RFP CEN)</i>	This study
SFNY2699	<i>MATα his3-200 leu2-3,112 ura3-52 atg13Δ::His3MX6 pLMB74 (URA3 GFP-SEC12 CEN) pSFNB2193 (LEU2 APE1-RFP CEN)</i>	This study
SFNY2700	<i>MATα his3Δ1 leu2Δ0 ura3Δ0 met15Δ0 hrr25Δ::KanMX6 APE1-RFP::His3MX6 pSFNB1871 (LEU2 hrr25-5 CEN) pLMB74 (URA3 GFP-SEC12 CEN)</i>	This study
SFNY2701	<i>MATα his3-200 leu2-3,112 ura3-52 ypt1-3 pLMB74 (URA3 GFP-SEC12 CEN) pSFNB2193 (LEU2 APE1-RFP CEN)</i>	This study
SFNY2702	<i>MATα his3Δ1 leu2Δ0 ura3Δ0 met15Δ0 hrr25Δ::KanMX6 pSFNB1871 (LEU2 hrr25-5 CEN) SEC13-GFP::URA3 atg1Δ::MET15 APE1-RFP::His3MX6</i>	This study
SFNY2703	<i>MATα his3-200 leu2-3,112 ura3-52 ypt1-3 SEC13-GFP::URA3 atg1Δ::His3MX6 pSFNB2193 (LEU2 APE1-RFP CEN)</i>	This study
NY405	<i>MATα ura3-52 sec4-8</i>	Novick Lab Collection
NY738	<i>MATα ura3-52 sec12-4</i>	Novick Lab Collection
NY2770	<i>MATα ura3-52 leu2-3,112 his3-Δ200 ypt31Δ::His3MX6 ypt32ts</i>	Novick Lab Collection

All yeast expression plasmids are *CEN*, except pRB58, which is 2μ . All genes are under their own promoters, except pLMB74, which uses the *MET25* promoter. More information about the *CEN* plasmids we used can be found in Sikorski and Hieter (1989). The following mutations were found in *hrr25-5*: T724C (S242P), A792G (silent), T839A (L280Q), A854T (D285V), A914G (D305G), A957G (silent), T1013A (L338Q), and C1047T (silent). The insertion of "A" at nucleotide position 1370 causes a frame shift that leads to the truncation of the protein at aa 462.

References

- Bhandari, D., J. Zhang, S. Menon, C. Lord, S. Chen, J.R. Helm, K. Thorsen, K.D. Corbett, J.C. Hay, and S. Ferro-Novick. 2013. Sit4p/PP6 regulates ER-to-Golgi traffic by controlling the dephosphorylation of COPII coat subunits. *Mol. Biol. Cell.* 24:2727–2738. <http://dx.doi.org/10.1091/mbc.E13-02-0114>
- Groesch, M.E., H. Ruohola, R. Bacon, G. Rossi, and S. Ferro-Novick. 1990. Isolation of a functional vesicular intermediate that mediates ER to Golgi transport in yeast. *J. Cell Biol.* 111:45–53. <http://dx.doi.org/10.1083/jcb.111.1.45>
- Lian, J.P., and S. Ferro-Novick. 1993. Bos1p, an integral membrane protein of the endoplasmic reticulum to Golgi transport vesicles, is required for their fusion competence. *Cell.* 73:735–745. [http://dx.doi.org/10.1016/0092-8674\(93\)90253-M](http://dx.doi.org/10.1016/0092-8674(93)90253-M)
- Sikorski, R.S., and P. Hieter. 1989. A system of shuttle vectors and yeast host strains designed for efficient manipulation of DNA in *Saccharomyces cerevisiae*. *Genetics.* 122:19–27.